Supporting Information for

Conformational and Environmental Determinants of RNA Solvation Dynamics: Roles of Intrinsic Flexibility, Allostery, and Protein Binding

Amrita Chakraborty[†], *Susmita Roy**[†]

[†] Department of Chemical Sciences, Indian Institute of Science Education and Research Kolkata, West Bengal 741246

* *Corresponding author*

*susmita.roy@iiserkol.ac.in

This PDF file includes:

Supporting Results

- Bulk salt concentration calculation
- Comparison of probability distribution of water's residence time around TAR RNA in BIV apo to complex state.
- Power-law fitting of solvation decay computed for BIV complex state
- Computing solvation correlation function and timescale prediction at 1ps resolution and timescale prediction
- Comparison of solvation correlation function, Cs(t), decay profiles for BIV TAR-TAT complex with varying trajectories
- Solvation dynamics calculated for HIV-2 TAR and HIV-2 TAR-TAT complex and respective timescale is predicated upon fitting the plots using triexponential function
- Periodic energy fluctuation and distance fluctuation happening coherently for HIV-2 Apo

- ❖ Decomposition of solvation energy relaxation into distinct self and cross terms for the HIV-2
- ❖ Comparing characterizations solvation environment for HIV-2 Apo vs complex

Supporting Figures: Figure S1-S8

Supporting Tables: Table S1-S8

Bulk salt concentration calculation:

Time-averaged bulk salt concentrations are calculated by taking the time-averaged ratio between the numbers of bulk ions to that of the number of bulk water molecules multiplied by the molarity of pure water. All species which are present beyond 2 nm of the RNA are considered to be bulk species according to the radial distribution function as depicted in **RDF plots**.

$$[\mathrm{Cl}^-]^* = 55.51M \left\langle \frac{B_{\mathrm{Cl}^-}}{B_{H_2O}} \right\rangle \qquad \text{(eq 1)}$$

$$[Na^+]^* = 55.51M \left\langle \frac{B_{\mathrm{NA}^+}}{B_{H_2O}} \right\rangle \qquad \text{(eq 2)}$$

From this raw concentration one has to determine the corrected concentration of the ionic species in the bulk following the relation as:

$$[j] = [j]^* \left\{ 1 - q_j \frac{\sum q_i [i^*]}{\sum q_i^2 [i^*]} \right\} \qquad \text{(eq 3)}$$

Here, q_j is the charge of the ionic species, $[j]^*$ and $[j]$ denotes the raw concentration and the corrected concentration, respectively. The bulk ionic concentration of NaCl for both the system was found to be within the range of 100±10mM, which is in the physiological ionic range. Details about the value of the ionic concentrations are given in **Table S1, S2, and S3**.

Table S1: Accounting for total number of surrounding species to the system

System	No. of Water molecule	No. of Sodium ion	Number of Chloride ion
BIV TAR RNA	56308	116	89
BIV TAR-TAT Complex	55974	116	97
HIV-2 TAR RNA	56003	133	104
HIV-2 TAR-TAT Complex	55920	125	104

Table S2: Accounting for bulk number of surrounding species to the system

System	No. of bulk Water molecule	No. of bulk Sodium ion	No. of bulk Chloride ion
BIV TAR RNA	50306.03	88.35	83.11
BIV TAR-TAT Complex	49911.18	94.24	90
HIV-2 TAR RNA	49868.86	101.11	96.52
HIV-2 TAR-TAT Complex	49688.44	111.93	107.27

Table S3: Accounting for corrected concentration of ions and preferential interaction coefficient

System	Ions	Rough concentration(mM)	Corrected Concentration(mM)	Preferential interaction coefficient
BIV TAR RNA	Na+ Cl-	97.49 91.71	94.51 94.51	20.13 -6.87
BIV TAR-TAT Complex	Na+ Cl-	104.81 100.1	102.4 102.4	12.75 -6.25
HIV-2 TAR RNA	Na+ Cl-	112.55 107.44	109.93 109.93	22.09 -6.91
HIV-2 TAR-TAT Complex	Na+ Cl-	111.93 107.27	109.55 109.55	14.64 -6.36

Comparison of probability distribution of water's residence time around TAR RNA in BIV apo to complex state:

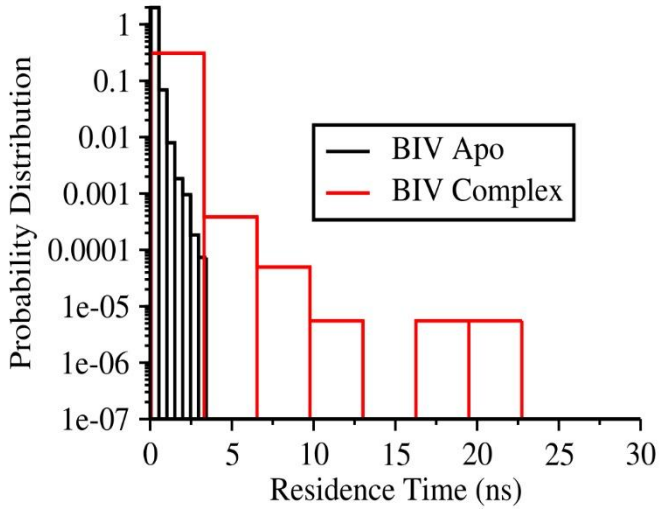

Figure S1: Comparison of the residence time of water molecules in the first solvation shell of BIV TAR RNA in the apo state versus the TAT-bound complex.

Power-law fitting of solvation decay computed for BIV complex state:

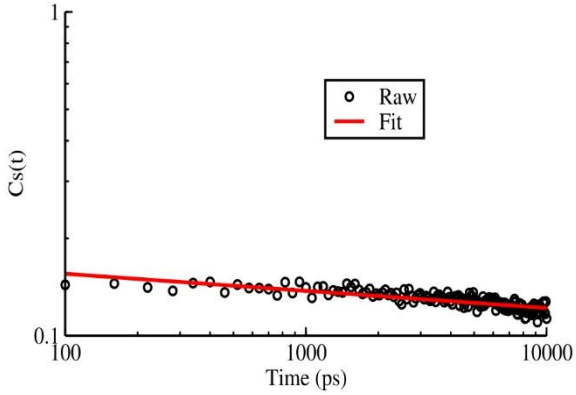

Figure S2: Power-law[1] fitting of the decay profile of the BIV TAR–TAT complex within the 100 ps to 10 ns time window (shown on a log–log scale).

Table S4: Fitting parameter for BIV TAR-TAT Complex (Power-Law)

a0	a1
0.198	0.0529

Computing solvation correlation function and timescale prediction at 1ps resolution and timescale prediction:

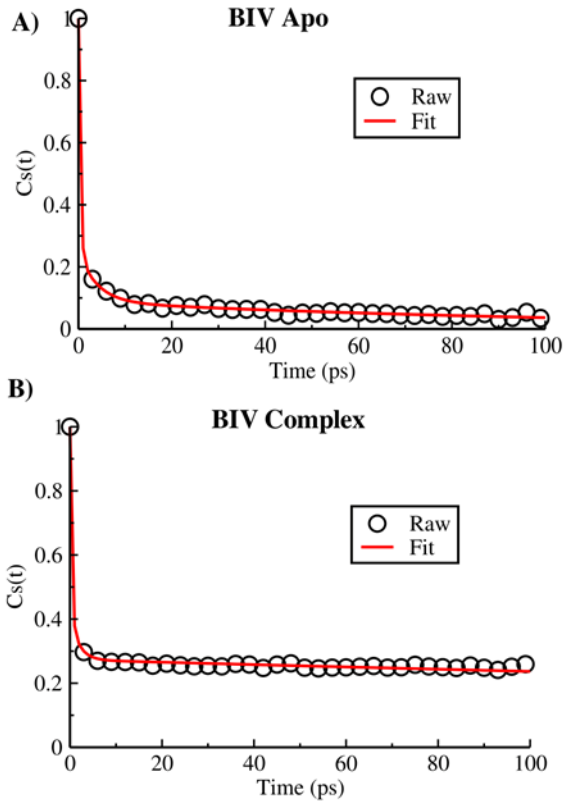

Figure S3: Multi-exponential fitting of BIV TAR solvation dynamics at 1 ps resolution for (A) the apo state and (B) the TAT-bound complex state.

Table S5: Fitting parameter for BIV Apo (Tri-exponential[2,3], resolution=1ps)

a1	a2	a3	T1	T2	T3	<T>
0.751	0.162	0.087	0.36 ps	4.02 ps	114.43 ps	10.88 ps

Table S6: Fitting parameter for BIV Complex (Tri-exponential[2,3], resolution=1ps)

a1	a2	a3	T1	T2	T3	<T>
0.589	0.138	0.273	0.32 ps	1.86 ps	700.0 ps	191.55 ps

Comparison of decay profiles for BIV TAR-TAT complex with varying trajectories:

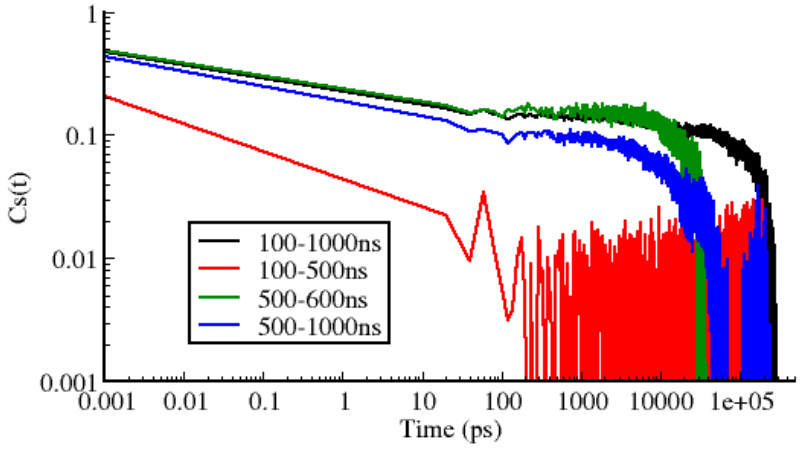

Figure S4: Comparison of solvation time-correlation function Cs(t) for the BIV TAR RNA in the TAT-bound complex, evaluated across trajectory segments of varying lengths (100–1000 ns, 100–500 ns, 500–600 ns, and 500–1000 ns).

Solvation dynamics calculated for HIV-2 TAR and HIV-2 TAR-TAT complex and respective timescale is predicated upon fitting the plots using triexponential function:

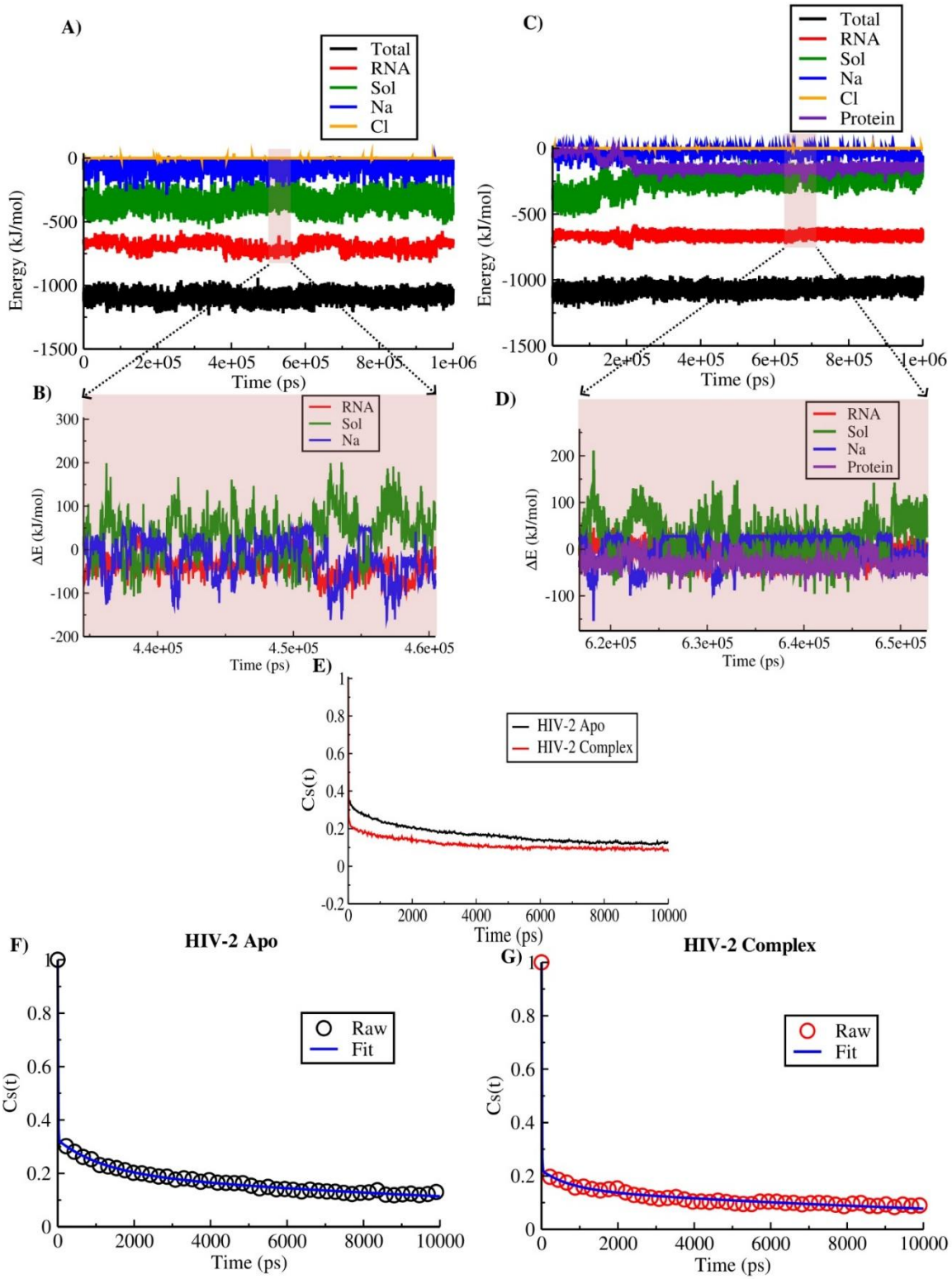

Figure S5: Decomposition of solvation energy relaxation into distinct environmental contributions for the HIV-2 TAR RNA in its apo and TAT-bound complex states.

(A) Probe–rest interaction energy along the trajectory for the HIV-2 apo RNA, shown as both the total contribution and its decomposition into individual components. (B) Enlarged view of panel (A), highlighting fluctuations in interaction energy (ΔE) for the RNA, solvent, and Na^+ ion components. (C) and (D) Same analyses as in panels (A) and (B), respectively, but for the HIV-2 TAR–TAT complex. (E) Comparative decay profiles of the solvation time-correlation function for the apo and complex systems at 20 ps resolution. (F) and (G) Triexponential fits to the solvation decay profiles for the apo and complex states, respectively.

Table S7: Fitting parameter for HIV-2 Apo (Tri-exponential, resolution=20ps)

a1	a2	a3	T1	T2	T3	<T>
0.675	0.122	0.203	7.38 ps	1184.66 ps	17377.2 ps	3677.08 ps

Table S8: Fitting parameter for HIV-2 Complex (Tri-exponential, resolution=20ps)

a1	a2	a3	T1	T2	T3	<T>
0.779	0.07	0.151	7.32 ps	746.97ps	15000 ps	2322.99 ps

Periodic energy fluctuation and distance fluctuation happening coherently for HIV-2 Apo:

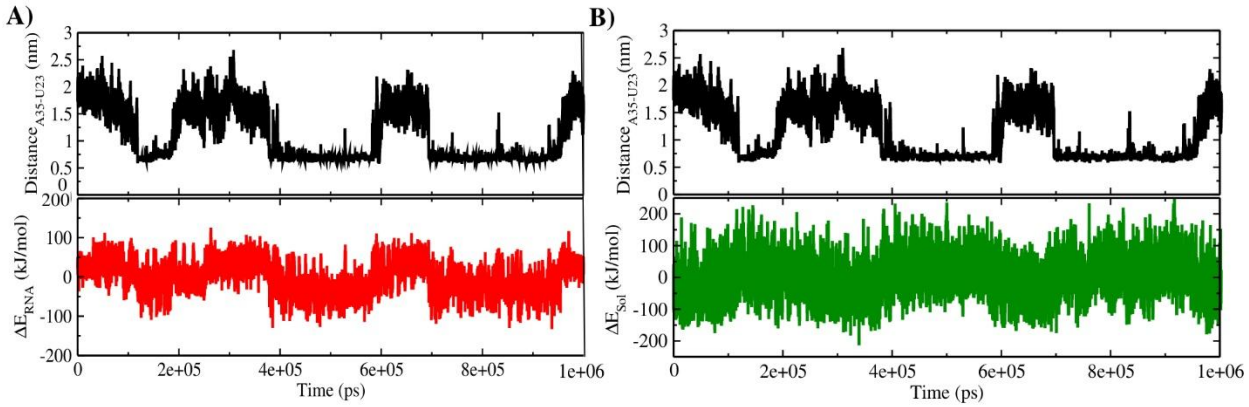

Figure S6: Time evolution of structural energy fluctuations and their coherent periodicity with the A35 distance fluctuation, illustrating a distal conformational response sensed by the probe.

Decomposition of solvation energy relaxation into distinct self and cross terms for the HIV-2:

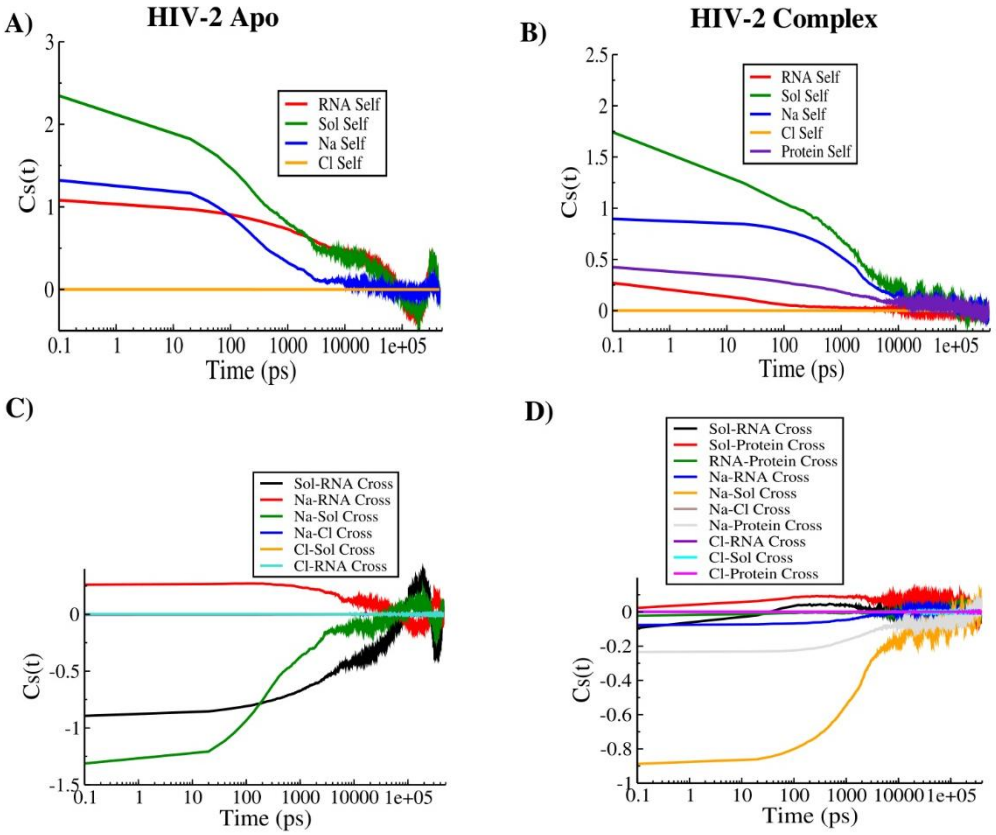

Figure S7: Linear-response decomposition[4,5] of the decay function of HIV-2 TAR RNA into self and cross terms. (A) and (B) Self-term and cross-term contributions of the individual components governing the decay in the HIV-2 apo TAR. (C) and (D) Corresponding self-term and cross-term decompositions for the HIV-2 TAR–TAT complex.

Comparing characterizations of solvation environment for HIV-2 Apo vs complex:

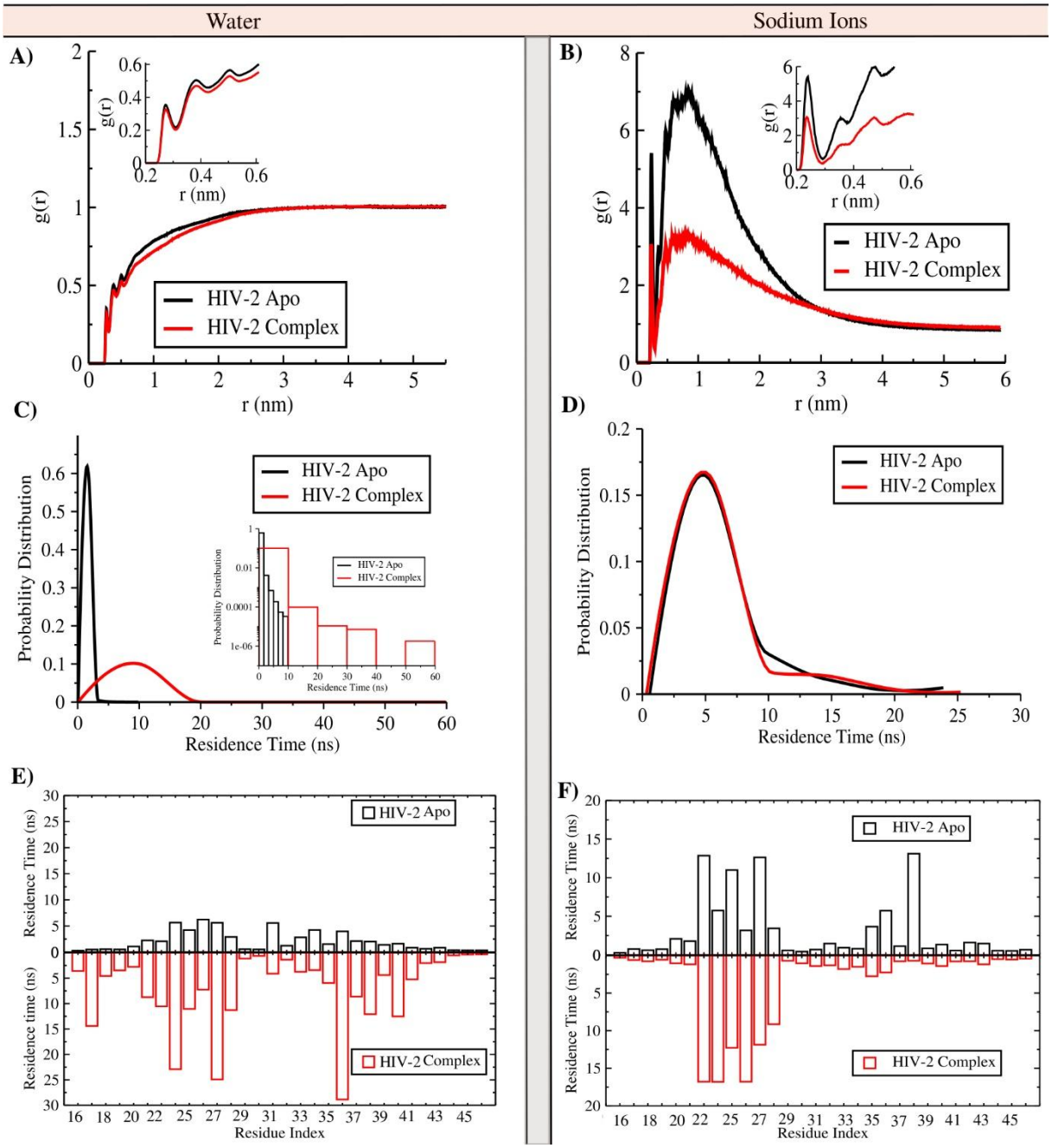

Figure S8: Characterization of the water and ion (Na^+) environment surrounding the RNA duplex in the apo and TAT-bound HIV-2 TAR states. (A) and (B) Radial distribution functions of water and Na^+ ions, respectively, around all RNA heavy atoms, shown in a comparative manner for the apo and complex forms. (C) and (D) Distributions of residence times for water and Na^+ ions within the first hydration shell (up to 3.5 Å) of the RNA in both states. (E) and (F) Changes

in the residue-wise maximum residence times of first-shell water and Na^+ ions, respectively, upon transition from the apo state to the TAT-bound complex.

References:

1 D. Andreatta, J. L. Pérez Lustres, S. A. Kovalenko, N. P. Ernsting, C. J. Murphy, R. S. Coleman and M. A. Berg, Power-law solvation dynamics in DNA over six decades in time, *J Am Chem Soc*, DOI:10.1021/ja044177v.

2 R. Jimenez, G. R. Fleming, P. V. Kumar and M. Maroncelli, Femtosecond solvation dynamics of water, *Nature*, DOI:10.1038/369471a0.

3 B. Bagchi and B. Jana, Solvation dynamics in dipolar liquids, *Chem Soc Rev*, DOI:10.1039/b902048a.

4 S. Pal, P. K. Maiti, B. Bagchi and J. T. Hynes, Multiple time scales in solvation dynamics of DNA in aqueous solution: The role of water, counterions, and cross-correlations, *Journal of Physical Chemistry B*, DOI:10.1021/jp065690t.

5 K. E. Furse and S. A. Corcelli, Molecular dynamics simulations of DNA solvation dynamics, *Journal of Physical Chemistry Letters*, DOI:10.1021/jz100485e.